Validation of Aura Microwave Limb Sounder Ozone by ozonesonde and lidar measurements

Y. B. Jiang, L. Froidevaux, A. Lambert, N. J. Livesey, W. G. Read, J. W. Waters, B. Bojkov, T. Leblanc, I. S. Mcdermid, Sophie Godin-Beekmann, et al.

Validation of Aura Microwave Limb Sounder Ozone by ozonesonde and lidar measurements

Y. B. Jiang,[1] L. Froidevaux,[1] A. Lambert,[1] N. J. Livesey,[1] W. G. Read,[1] J. W. Waters,[1] B. Bojkov,[2] T. Leblanc,[3] I. S. McDermid,[3] S. Godin-Beekmann,[4] M. J. Filipiak,[5] R. S. Harwood,[5] R. A. Fuller,[1] W. H. Daffer,[1] B. J. Drouin,[1] R. E. Cofield,[1] D. T. Cuddy,[1] R. F. Jarnot,[1] B. W. Knosp,[1] V. S. Perun,[1] M. J. Schwartz,[1] W. V. Snyder,[1] P. C. Stek,[1] R. P. Thurstans,[1] P. A. Wagner,[1] M. Allaart,[6] S. B. Andersen,[7] G. Bodeker,[8] B. Calpini,[9] H. Claude,[10] G. Coetzee,[11] J. Davies,[12] H. De Backer,[13] H. Dier,[14] M. Fujiwara,[15] B. Johnson,[16] H. Kelder,[6] N. P. Leme,[17] G. König-Langlo,[18] E. Kyro,[19] G. Laneve,[20] L. S. Fook,[21] J. Merrill,[22] G. Morris,[23] M. Newchurch,[24] S. Oltmans,[16] M. C. Parrondos,[25] F. Posny,[26] F. Schmidlin,[27] P. Skrivankova,[28] R. Stubi,[9] D. Tarasick,[12] A. Thompson,[29] V. Thouret,[30] P. Viatte,[9] H. Vömel,[31] P. von Der Gathen,[32] M. Yela,[25] and G. Zablocki[33]

Received 10 April 2007; revised 2 August 2007; accepted 31 October 2007; published 15 December 2007.

[1] We present validation studies of MLS version 2.2 upper tropospheric and stratospheric ozone profiles using ozonesonde and lidar data as well as climatological data. Ozone measurements from over 60 ozonesonde stations worldwide and three lidar stations are compared with coincident MLS data. The MLS ozone stratospheric data between 150 and 3 hPa agree well with ozonesonde measurements, within 8% for the global average. MLS values at 215 hPa are biased high compared to ozonesondes by ~20% at middle to high latitude, although there is a lot of variability in this altitude region. Comparisons between MLS and ground-based lidar measurements from Mauna Loa, Hawaii, from the Table Mountain Facility, California, and from the Observatoire de Haute-Provence, France, give very good agreement, within ~5%, for the stratospheric values. The comparisons between MLS and the Table Mountain Facility tropospheric ozone lidar show that MLS data are biased high by ~30% at 215 hPa, consistent with that indicated by the ozonesonde data. We obtain better global average agreement between MLS and ozonesonde partial column values down to 215 hPa, although the average MLS values at low to middle latitudes are higher than the ozonesonde values by up to a few percent. MLS

[1]Jet Propulsion Laboratory, California Institute of Technology, Pasadena, California, USA.
[2]NASA Goddard Space Flight Center, Greenbelt, Maryland, USA.
[3]Jet Propulsion Laboratory, California Institute of Technology, Table Mountain Facility, Wrightwood, California, USA.
[4]Service d'Aeronomie/Institut Pierre-Simon Laplace, Centre National de la Recherche Scientifique–Université Pierre et Marie Curie, Paris, France.
[5]Institute of Atmospheric and Environmental Science, University of Edinburgh, Edinburgh, UK.
[6]Royal Netherlands Meteorological Institute, de Bilt, Netherlands.
[7]Danish Meteorological Institute, Copenhagen, Denmark.
[8]National Institute of Water and Atmospheric Research, Lauder, New Zealand.
[9]Aerological Station Payerne, MeteoSwiss, Payerne, Switzerland.
[10]Meteorological Observatory Hohenpeissenberg, German Weather Service, Hohenpeissenberg, Germany.
[11]South African Weather Service, Irene, South Africa.
[12]Environment Canada, Downsview, Ontario, Canada.
[13]Royal Meteorological Institute of Belgium, Brussels, Belgium.
[14]Meteorological Observatory Lindenberg, German Weather Service, Lindenberg, Germany.
[15]Graduate School of Environmental Earth Science, Hokkaido University, Sapporo, Japan.
[16]Global Monitoring Division, Earth System Research Laboratory, NOAA, Boulder, Colorado, USA.
[17]Laboratorio De Ozonio, Instituto Nacional de Pesquisas Espaciais, Sao Paulo, Brazil.
[18]Alfred Wegener Institute for Polar and Marine Research, Bremerhaven, Germany.
[19]Arctic Research Center, Finnish Meteorological Institute, Sodankyla, Finland.
[20]Centro di Ricerca Progetto San Marco, Università degli Studi di Roma "La Sapienza," Rome, Italy.
[21]Malaysian Meteorological Service, Petaling Jaya, Selangor, Malaysia.
[22]Graduate School of Oceanography, University of Rhode Island, Narragansett, Rhode Island, USA.
[23]Department of Physics and Astronomy, Valparaiso University, Valparaiso, Indiana, USA.
[24]Atmospheric Science Department, University of Alabama–Huntsville, Huntsville, Alabama, USA.
[25]National Institute for Aerospace Technology, Madrid, Spain.
[26]Laboratoire de l'Atmosphère et des Cyclones, La Réunion, France.
[27]NASA Goddard Space Flight Center, Wallops Island, Virginia, USA.
[28]Czech Hydrometeorological Institute, Prague, Czech Republic.
[29]Department of Meteorology, Pennsylvania State University, State College, Pennsylvania, USA.
[30]Laboratoire d'Aerologie, Centre National de la Recherche Scientifique, Toulouse, France.
[31]Cooperative Institute for Research in Environmental Science, University of Colorado, Boulder, Colorado, USA.
[32]Alfred Wegener Institute, Potsdam, Germany.

0148-0227/07/2007JD008776

v2.2 ozone data agree better than the MLS v1.5 data with ozonesonde and lidar measurements. MLS tropical data show the wave one longitudinal pattern in the upper troposphere, with similarities to the average distribution from ozonesondes. High upper tropospheric ozone values are also observed by MLS in the tropical Pacific from June to November.

Citation: Jiang, Y. B., et al. (2007), Validation of Aura Microwave Limb Sounder Ozone by ozonesonde and lidar measurements, *J. Geophys. Res.*, *112*, D24S34, doi:10.1029/2007JD008776.

1. Introduction

[2] The Microwave Limb Sounder (MLS) is one of four instruments on the Earth Observing System (EOS) Aura satellite which was launched on 15 July 2004 and placed into a near-polar orbit at ~705 km altitude, with a ~1:45 p.m. ascending equatorial crossing time. The Aura mission objectives are to study the Earth's ozone, air quality, and climate [*Schoeberl et al.*, 2006a, 2006b]. MLS [*Waters et al.*, 1999, 2006] contributes to this objective by measuring atmospheric temperature profiles from the troposphere to the thermosphere, and more than a dozen atmospheric constituent profiles, as well as cloud ice water content [*Wu et al.*, 2006] from millimeter- and submillimeter-wavelength thermal emission of Earth's limb with seven radiometers covering five broad spectral regions.

[3] Initial ozone validation results using MLS v1.5 data include the early work of *Froidevaux et al.* [2006], as well as results of comparisons between MLS and ground-based microwave profiles [*Hocke et al.*, 2006], and the analyses of *Ziemke et al.* [2006] and D. Yang et al. (Midlatitude tropospheric ozone columns derived from Aura OMI and MLS data using the TOR approach and mapping techniques, submitted to *Journal of Geophysical Research*, 2007, hereinafter referred to as Yang et al., submitted manuscript, 2007), focusing on stratospheric columns and resulting tropospheric ozone residual column abundances, using a combination of MLS and OMI data.

[4] In this paper, we present validation results of the newly released MLS version 2.2 (or v2.2) ozone product from the upper troposphere to the upper stratosphere through comparisons with global ozonesonde and ground-based lidar measurements. Although MLS measures ozone in several spectral bands [*Waters et al.*, 1999, 2006], this paper focuses on the "MLS standard product" for ozone, which is obtained from radiance measurements near 240 GHz and provides the best overall precision for the widest vertical range. There are related papers focusing on validation of the 240 GHz MLS ozone (and CO) data in the upper troposphere and lower stratosphere [*Livesey et al.*, 2007], mainly for pressures of 100 hPa and larger, and in the stratosphere and lower mesosphere (L. Froidevaux et al., Validation of Aura Microwave Limb Sounder Stratospheric ozone measurements, submitted to *Journal of Geophysical Research*, 2007, hereinafter referred to as Froidevaux et al., submitted manuscript, 2007), using satellite, aircraft and ground-based ozone measurements. Version 2.2 is currently in the early stages of reprocessing and is therefore more limited in terms of available days than version 1.5, with about 3 months of v2.2 reprocessed data, covering selected days in 2004, 2005, and 2006. A recent minor software patch has led to version 2.21, with results that are essentially identical to v2.20 results for the vast majority of days.

[5] In section 2, we summarize the data usage and screening recommendations for MLS v2.2 ozone profiles. Section 2 also provides a brief description of the estimated MLS ozone uncertainties, both random and systematic, which we generally refer to as precision and accuracy. We provide the comparisons between MLS ozone and ozonesonde profiles in section 3, followed by section 4 on ground-based lidar measurement comparisons. Section 5 summarizes the results and suggests improvements needed in future versions.

2. MLS Ozone Measurements

[6] For an overview of the MLS spectral bands, main line frequencies, and target molecules, see *Waters et al.* [2006]. The overall MLS retrieval approach is discussed by *Livesey et al.* [2005, 2006] and the calculation specifics of the MLS radiance model (or "forward model") are described by *Read et al.* [2006] and *Schwartz et al.* [2006]. MLS radiance spectra and residuals are discussed by *Livesey et al.* [2007] and Froidevaux et al. (submitted manuscript, 2007), who show that the radiance fits are generally very good (within ~1%) although there is typically poorer closure in the lowermost height region (upper troposphere).

2.1. Data Usage and Screening

[7] The MLS v2.2 ozone data files provide the ozone abundance fields as well as the estimated (single profile) precision fields and related data screening flags. The recommendations for screening the MLS v2.2 ozone profiles are similar but not identical to those given by *Livesey et al.* [2005] for version 1.5 data. A detailed illustration of these data screening fields is given by *Livesey et al.* [2005] for MLS v1.5 data. We recommend the use of only even values of the "Status" field. Also there is now a slightly different threshold value for the "Quality" flag, which refers to the overall radiance fit for each profile; users should use only Quality > 0.4 for the stratosphere (Froidevaux et al., submitted manuscript, 2007) and Quality > 1.2 for the upper troposphere [*Livesey et al.*, 2007]; we have conservatively used the Quality > 1.2 in this work. A new field named "Convergence" is also used in v2.2, and it refers to the ratio of the radiance fit chi-square value for each profile to the chi-square value that the retrieval would have been expected to reach. Users should retain only ozone profiles with Convergence < 1.8, which eliminates only about 1% of the available daily ozone profiles.

[8] The data usage guidelines for MLS v2.2 ozone are summarized in Table 1. While more work of a very detailed nature is needed to further refine the data screening recom-

Table 1. MLS v2.2 Ozone Data Usage Guidelines

Flag	Meaning/Usage	Values to Use
Status	can indicate operational or retrieval problems, and possible influence of clouds	even
Quality	radiance fit by the retrieval algorithms	>0.4 (stratosphere), >1.2 (upper troposphere)
Convergence (new for v2.2)	ratio of the radiance fit to that expected by the retrieval algorithms	<1.8
Precision	negative if large contribution of a priori to the retrieved value	>0
Pressure range	useful vertical range	215–0.02 hPa

mendations provided above, these recommendations will generally safely allow for the use of more than roughly 97% of the available daily MLS ozone profiles. As the retrievals at pressures larger than 215 hPa are not deemed satisfactory enough at this time [*Livesey et al.*, 2007], we will only consider ozone at pressures of 215 hPa or less in the following comparisons.

2.2. Resolution, Precision, and Accuracy

[9] As described for atmospheric retrievals by *Rodgers* [1976], the vertical and horizontal (along the MLS suborbital track) resolutions can be visualized through the use of the averaging kernel matrix. The averaging kernels for ozone have values very close to unity and are sharply peaked; the influence of a priori profile information on the retrievals is negligible [*Livesey et al.*, 2007; Froidevaux et al., submitted manuscript, 2007]. The vertical resolution is 2.7 to 3 km from the upper troposphere to the lower mesosphere.

[10] The precision of the MLS ozone profiles is estimated by the MLS retrieval calculations, following the *Rodgers* [1976] formulation; these uncertainty estimates are provided in the MLS Level 2 files (for each profile), as the diagonal values of the error covariance matrix. The estimated root

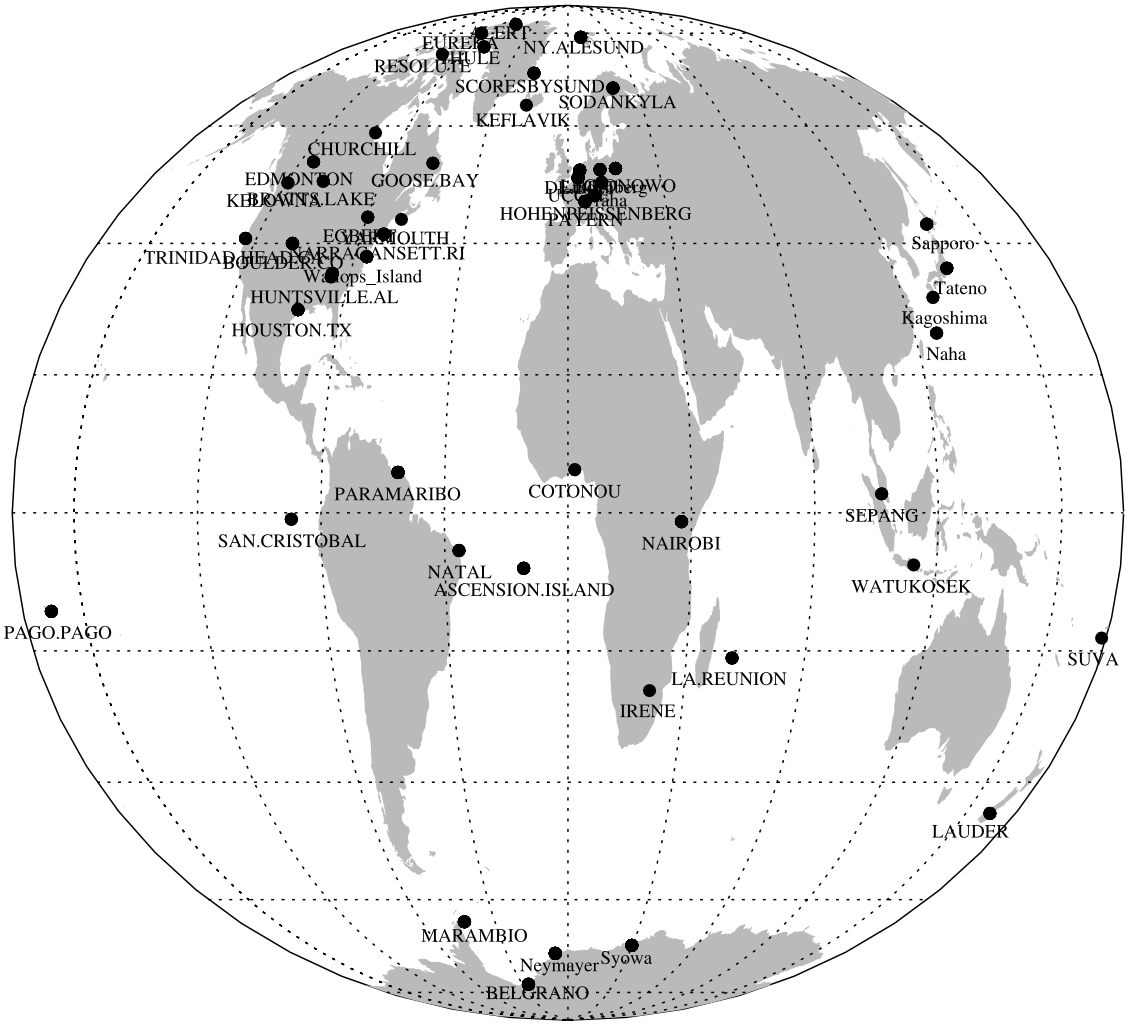

Figure 1. Global distribution of ozonesonde stations considered in this work.

Table 2. Ozonesonde Site Information for Comparisons Used in This Work

Site Name	Latitude	Longitude	Contact or Data Source	Number of Coincident Profiles With Aura MLS
Alert (NU), Canada	82.50	−62.33	D. Tarasick/J. Davies (EC/MSC)	2
Ascension Island, United Kingdom	−7.98	−14.42	F. Schmidlin (NASA/GSFC)	30
Belgrano (Argentina), Antarctica	−77.85	−34.55	M. Yela (INTA)	15
Boulder (CO), USA	40.00	−105.25	S. Oltmans/B. Johnson (NOAA/ESRL)	25
Bratts Lake (SK), Canada	50.20	−104.70	D. Tarasick/J. Davies (EC/MSC)	7
Churchill (MB), Canada	58.74	−94.07	D. Tarasick/J. Davies (EC/MSC)	8
Cotonou, Benin	6.21	2.23	A. Thompson (PSU), V. Thouret (CNRS/LA)	16
De Bilt, Netherlands	52.10	5.18	M. Allaart (KNMI)	36
Edmonton (AB), Canada	53.55	−114.11	D. Tarasick/J. Davies (EC/MSC)	9
Egbert (ON), Canada	44.23	−79.78	D. Tarasick/J. Davies (EC/MSC)	10
Eureka (NU), Canada	79.99	−85.94	D. Tarasick/J. Davies (EC/MSC)	4
Goose.Bay (NF), Canada	53.31	−60.36	D. Tarasick/J. Davies (EC/MSC)	15
Heredia, Costa Rica	10.00	−84.10	H. Vömel (NOAA/ESRL)	4
Hilo (HI), USA	19.43	−155.04	S. Oltmans/B. Johnson (NOAA/ESRL)	10
Hohenpeissenberg, Germany	47.80	11.00	H. Claude (DWD)	92
Houston (TX), USA	29.72	−95.40	G. Morris (Valparaiso U.)	6
Huntsville (AL), USA	35.28	−86.59	S. Oltmans (NOAA/ESRL), M. Newchurch (U. Alabama-Huntsville)	31
Irene, South Africa	−25.90	28.22	A. Thompson (PSU), G. Coetzee (SAWS)	11
Jokioinen, Finland	60.80	23.50	E. Kyro (FMI)	13
Kagoshima, Japan	31.60	130.60	JMA, WOUDC	5
Keflavik, Iceland	63.97	−22.60	M. C. Parrondos (INTA)	16
Kelowna (BC), Canada	49.93	−119.40	D. Tarasick/J. Davies (EC/MSC)	7
La Reunion, France	−21.06	55.48	F. Posny (U. de La Reunion)	18
Lauder, New Zealand	−45.04	169.68	G. Bodeker (NIWA)	32
Legionowo, Poland	52.40	20.97	Grzegorz Zablocki (IMGW)	40
Lindenberg, Germany	52.20	14.10	Horst Dier (DWD)	17
Malindi, Kenya	−2.99	40.19	A. Thompson (PSU), G. Laneve (U. Rome)	7
Marambio (Argentina), Antarctica	−56.72	−64.23	E. Kyro (FMI)	25
Naha (Okinawa), Japan	26.20	127.70	JMA, WOUDC	11
Nairobi, Kenya	−1.27	36.80	B. Calpini (MeteoSwiss)	28
Narragansett (RI), USA	41.49	−71.42	S. Oltmans/B. Johnson (NOAA/ESRL), J. Merrill (U. Rhode Island)	25
Natal, Brazil	−5.42	−35.38	N. P. Leme (INPE), F. Schmidlin (NASA GSFC)	21
Neumayer, Antactica	−70.70	−8.30	G. König-Langlo (AWI)	24
Ny Aalesund (Spitsbergen), Norway	78.93	11.95	P. von Der Gathen (AWI)	6
Pago Pago, American Samoa	−14.23	−170.56	S. Oltmans/B. Johnson (NOAA/ESRL)	21
Paramaribo, Suriname	5.81	−55.21	H. Kelder (KNMI)	14
Payerne, Switzerland	46.80	7.00	P. Viatte/R. Stubi (MeteoSwiss)	102
Praha, Czech Republic	50.00	14.45	P. Skrivankova (CHMI)	20
Resolute (NU), Canada	74.71	−94.97	D. Tarasick/J. Davies (EC/MSC)	2
San Cristobal (Galapagos), Ecuador	−0.92	−89.60	S. Oltmans/B. Johnson (NOAA/ESRL)	11
Sapporo, Japan	43.10	141.30	JMA, WOUDC	15
Scoresbysund, Greenland	70.50	−22.00	S. B. Andersen (DMI)	16
Sepang (Kuala Lumpur), Malysia	2.73	101.70	A. Thompson (PSU), C.P. Leong (MMS)	8
Sodankyla, Finland	67.39	26.65	E. Kyro (FMI)	34
Summit, Greenland	72.60	−38.50	S. Oltmans/B. Johnson (NOAA/ESRL)	3
Suva, Fiji	−18.13	178.40	S. Oltmans/B. Johnson (NOAA/ESRL)	5
Syowa, Japan	−69.00	39.60	JMA, WOUDC	21
Tateno, Japan	36.10	140.10	JMA, WOUDC	13
Thule, Greenland	76.50	−68.70	S. B. Andersen (DMI)	2
Trinidad Head (CA), USA	40.80	−124.16	S. Oltmans/B. Johnson (NOAA/ESRL)	9
Uccle, Belgium	50.80	4.35	H.De Backer (KMI)	91
Wallops Island (VA), USA	37.90	−75.50	F. Schmidlin (NASA GSFC)	14
Watukosek (Java), Indonesia	−7.50	112.60	A. Thompson (PSU), M. Fujiwara (U. Hokkaido)	6
Yarmouth (NS), Canada	43.87	−66.11	D. Tarasick/J. Davies (EC/MSC)	10

mean square precision for MLS ozone retrievals is typically fairly constant as a function of latitude; precision values can be as low as 20 to 30 ppbv from 100 to 215 hPa, and increase by an order of magnitude (∼0.3 ppmv) near 1 hPa [*Livesey et al.*, 2007; Froidevaux et al., submitted manuscript, 2007].

[11] Simulation results for MLS ozone point to possible biases of about 5 to 10% (or 0.05 to 0.2 ppmv) for most of the stratosphere, down to 100 hPa, with precision (random errors on single profiles) of 2 to 30% (Froidevaux et al., submitted manuscript, 2007). Expected uncertainties increase, in percent, for MLS vertical retrieval grid pressures of 147 and 215 hPa, especially in the tropics, where ozone abundances are low [*Livesey et al.*, 2007].

3. Comparisons of MLS and Ozonesonde Data

[12] Ozonesondes are balloon-borne in situ instruments that continuously measure the ozone concentration as they ascend or descend in the atmosphere. A profile of ozone is

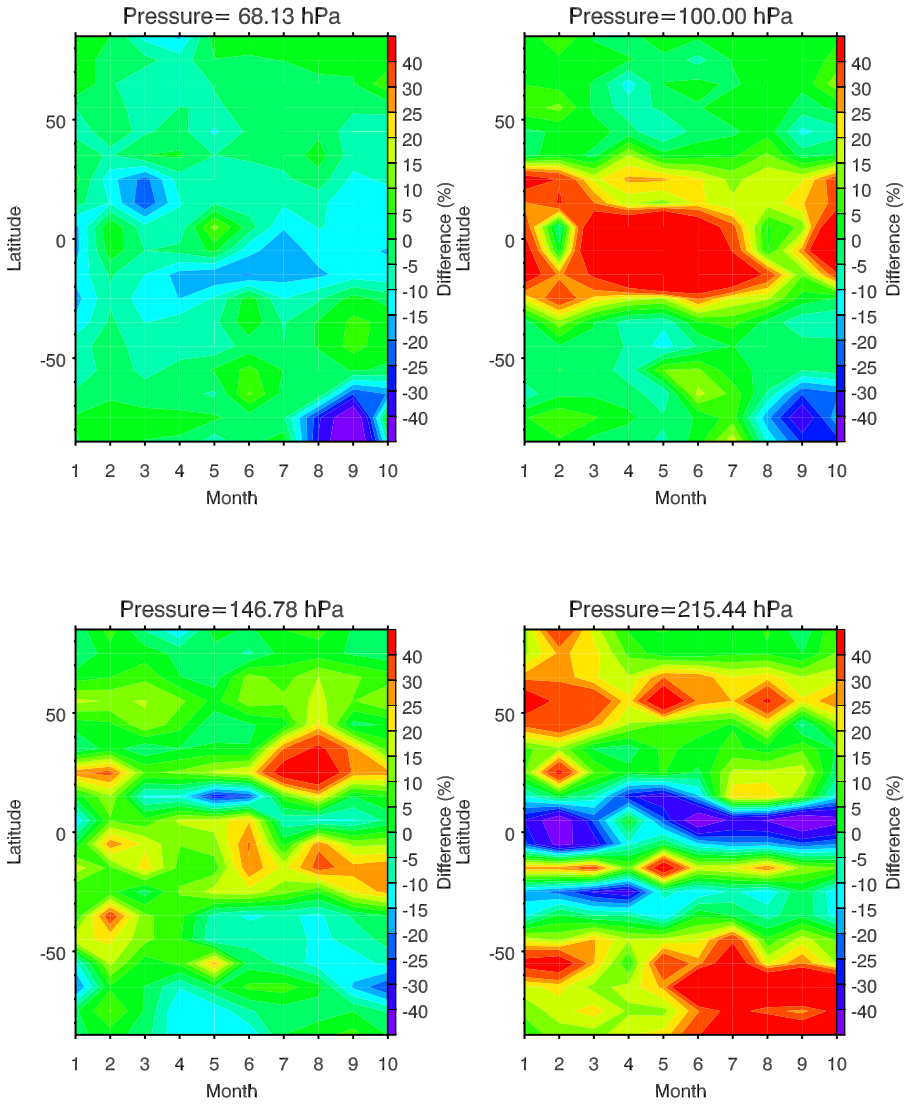

Figure 2. Comparisons between MLS v2.2 ozone and LLM climatology [*McPeters et al.*, 2007] in UT/LS at four pressure levels from January to October. The difference in percentage is defined as 100 * (MLS-LLM)/LLM.

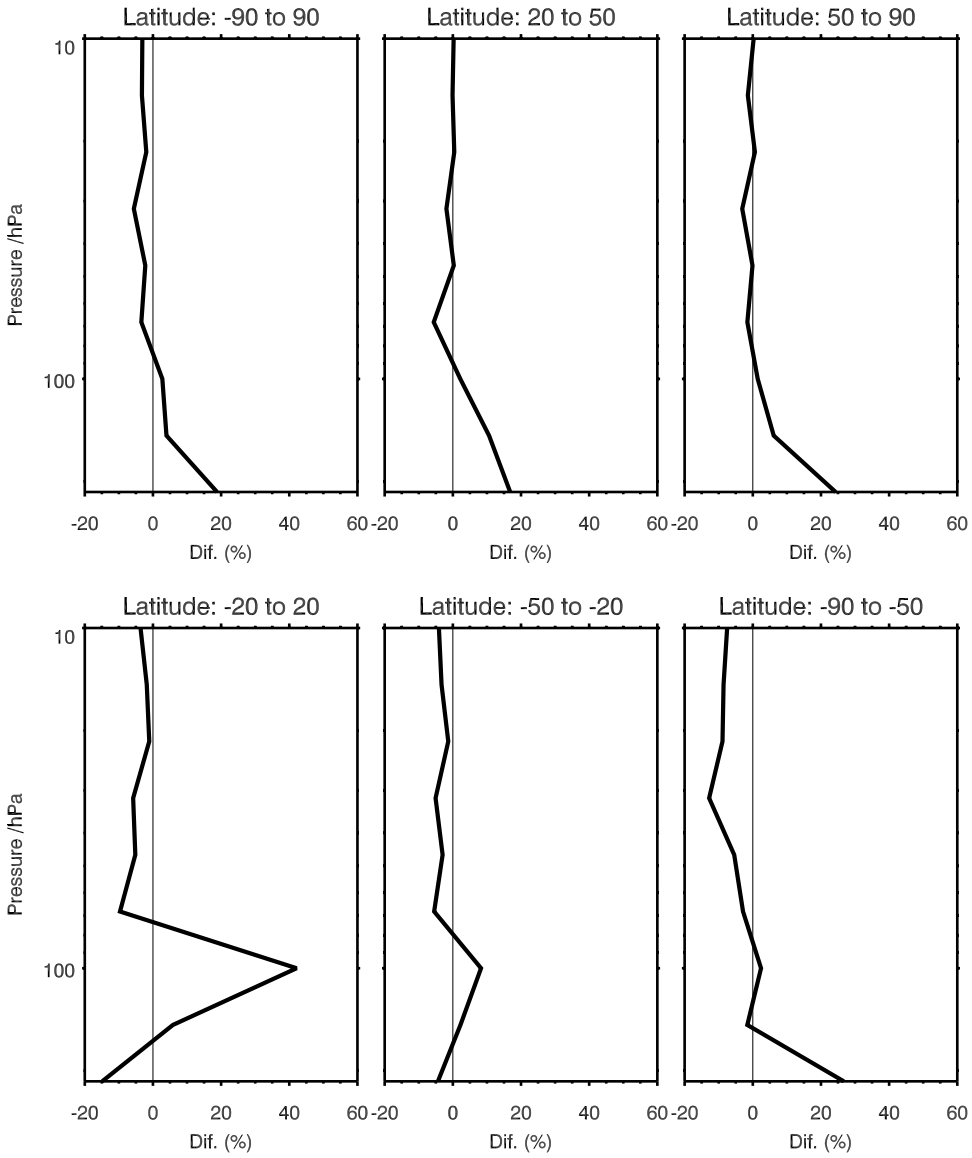

Figure 3. Comparisons between MLS v2.2 ozone and LLM climatology [*McPeters et al.*, 2007] in six latitude bins. The solid line represents the averaged percentage differences 100 * ((MLS-LLM)/LLM) between v2.2 and LLM climatology.

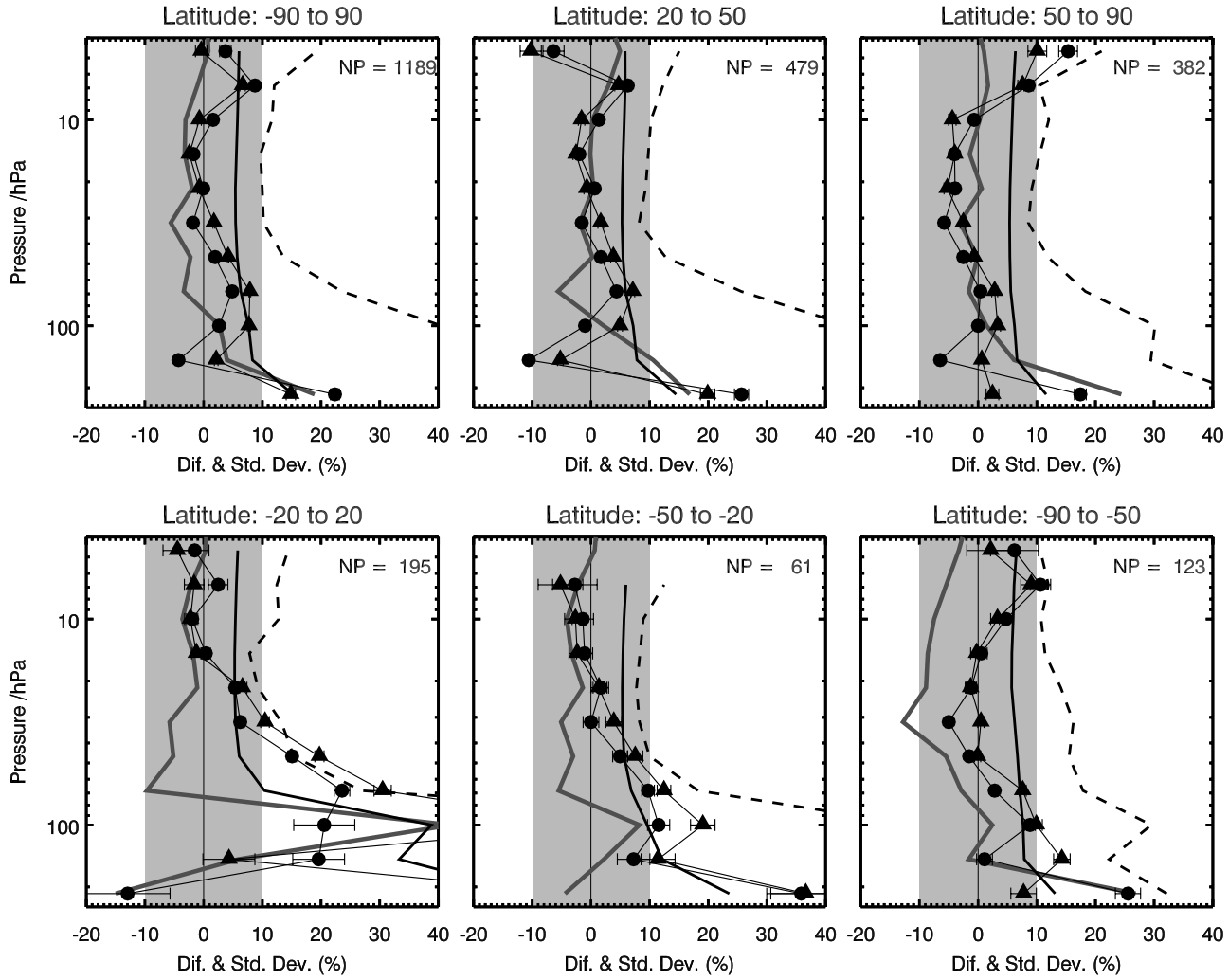

Figure 4. Comparisons between MLS v2.2, v1.5 ozone and ozonesonde measurements in 6 latitude bins. Solid circle and connected line represents the averaged percentage differences (100 * (MLS-Sonde)/Sonde) between v2.2 and ozonesondes, while solid triangle and connected line shows the averaged percentage differences between v1.5 and ozonesondes. Dashed line gives the standard deviation of the differences (in percent) between v2.2 and ozonesondes. Heavy solid line shows the combined precisions (in percent) for v2.2 and ozonesondes, using 5% precision for the sondes. The error bar on each data point (dot) is twice the precision in the mean differences (and is often too small to see). The solid dark gray line represents the averaged percentage differences (100 * (MLS-LLM)/LLM) between v2.2 and LLM climatology.

obtained up to the burst point of the balloon, often at altitude in excess of 30 km or a pressure as low as 5 to 10 hPa. Ozonesonde measurements are the most accurate means of providing high vertical resolution ozone profiles. The detection limit is typically less than 2 ppbv, as compared to the typical clean background value of 30 ppbv for tropospheric ozone. Measurement uncertainty is about 10% in the troposphere, 5% in the stratosphere up to 10 hPa and 5–25% between 10 and 3 hPa [*Bodeker et al.*, 1998; *Borchi et al.*, 2005; *Kerr et al.*, 1994; *Smit et al.*, 2007; *Thompson et al.*, 2007a, 2007b, 2007c; *World Climate Research Programme*, 1998]. We have used ozonesonde measurements available from the Aura Validation Data Center (AVDC) as well as some soundings from the World Ozone and Ultraviolet Data Center (WOUDC) in Toronto (http://www.woudc.org/). More than 70 stations were considered in this study, but considering the criteria we use to select the MLS and correlative data profiles and the availability of v2.2 and sonde data at the time of writing, some of the potentially available comparisons are currently missing. Figure 1 shows the global distribution of these stations. There is good coverage in the Northern Hemisphere high latitude, but the Southern Hemisphere coverage is sparse: only 4 stations at high southern latitudes, and 1 (Lauder, New Zealand) at the southern midlatitudes. The tropical stations are mainly from the Southern Hemisphere Additional Ozonesondes (SHADOZ) project. The ozonesonde sites and number of coincident profiles with MLS observations (when more than one exists) are listed in Table 2, with most of the data made available at the Aura Validation Data Center (AVDC); data from the sites labeled WOUDC were obtained directly from the WOUDC. Examination of ozo-

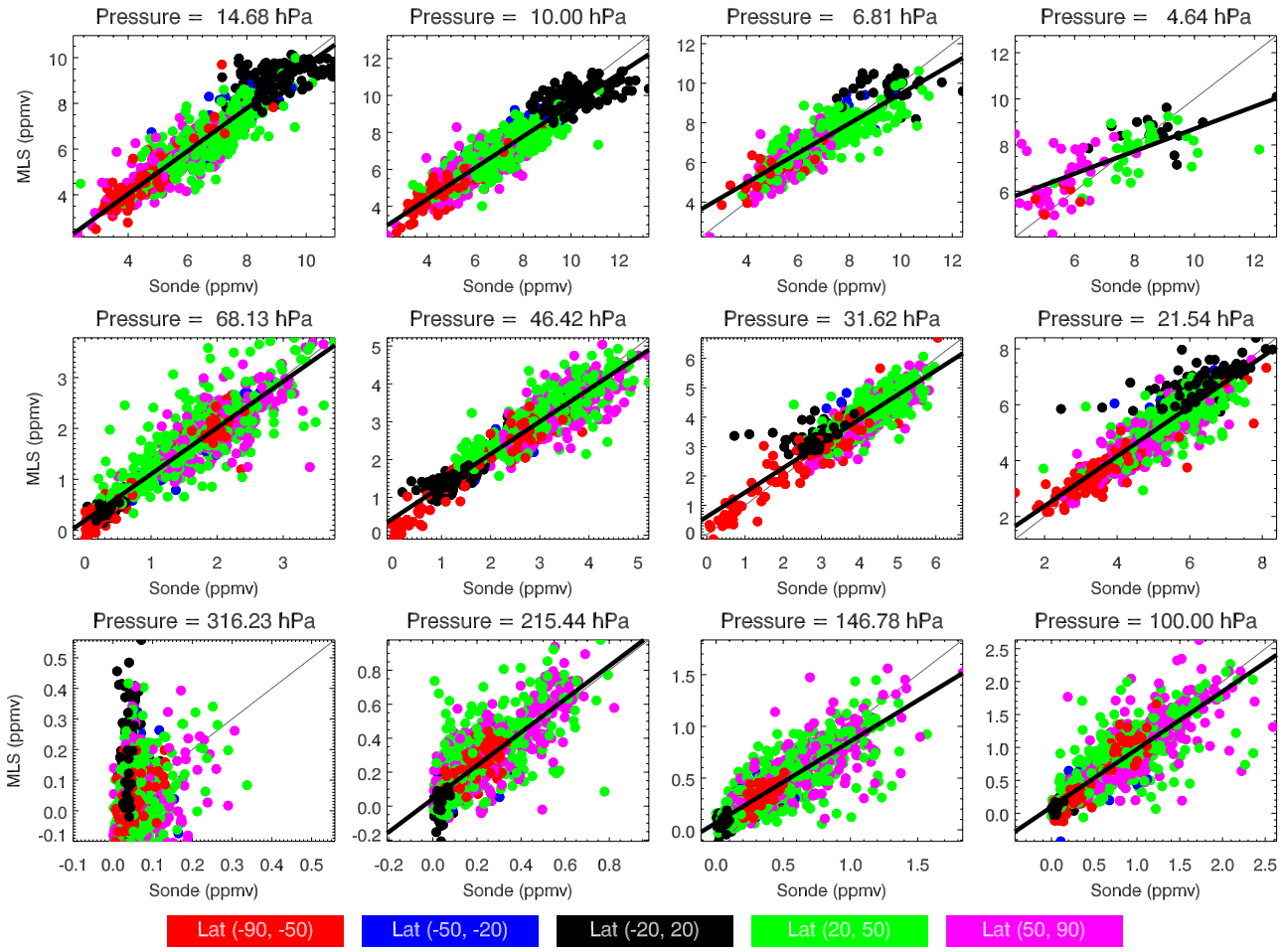

Figure 5. Scatterplots of MLS versus ozonesondes from all the stations for all the coincidences on selected pressure levels, color-coded in five latitude bins. The heavy black lines are the linear fits to the data.

nesonde measurements suggests that station-to-station biases exist between the different sites because of differences in data processing technique and sensor solution and varying hardware [*Johnson et al.*, 2002; *Thompson et al.*, 2003; *Smit et al.*, 2007].

[13] In order to get good statistics, we chose coincident MLS and ozonesonde profiles to be within ±2° latitude, ±10° longitude and on the same (GMT) day. We have looked at the comparisons using tighter criteria and while these results improve slightly (by 5% or less), this will not affect the main conclusions given here. In the comparisons, we have filtered the MLS data as pointed out in section 2.1, and used only cloud free profiles, based on the MLS cloud screening criteria (Status = 0). There are total 1196 profiles found in 2004, 2005 and 2006 based on the coincidences between MLS v2.2 and ozonesonde profiles. We have degraded the high-resolution ozonesonde profiles by using two methods: a least squares fit of the fine resolution pressure grid to the MLS ozone retrieval grid, and also, the use of MLS averaging kernels to smooth the ozonesonde data after the least squares fit to the MLS grid. There are negligible differences between the two methods, and the results of comparisons are not very sensitive to the method chosen, as expected, because of the sharply peaked nature of the MLS averaging kernels. We have used the averaging kernel method to degrade the ozonesonde high-resolution profiles throughout this work.

[14] In order to check the bias of MLS ozone versus climatology, we show comparisons between MLS v2.2 ozone and LLM climatology [*McPeters et al.*, 2007] in upper troposphere at four pressure levels in Figure 2. At the time of writing, there are no more than 10 days of MLS v2.2 data in August, November and December. We plot only January to October with interpolated August data. The LLM climatology combines data from the Stratospheric Aerosol and Gas Experiment II (SAGE II; 1988–2001), the Upper Atmosphere Research Satellite Microwave Limb Sounder (MLS; 1991–1999), and ozonesondes (1988–2002). At 68 hPa (and lower pressures, not shown), the comparison gives agreement within 5%, with a few places such as Antarctic ozone hole where MLS values are 10–20% lower than LLM. At the upper tropospheric levels, MLS values oscillate about the LLM climatology. At 100 hPa, MLS ozone is larger by as much as ~40% in the tropical region and lower by ~30% in the Antarctic ozone hole. While MLS ozone biases are lower (~20%) in the tropics and higher (~20%) in the higher latitude in both hemispheres at 215 hPa level. The MLS shows better agreement with LLM

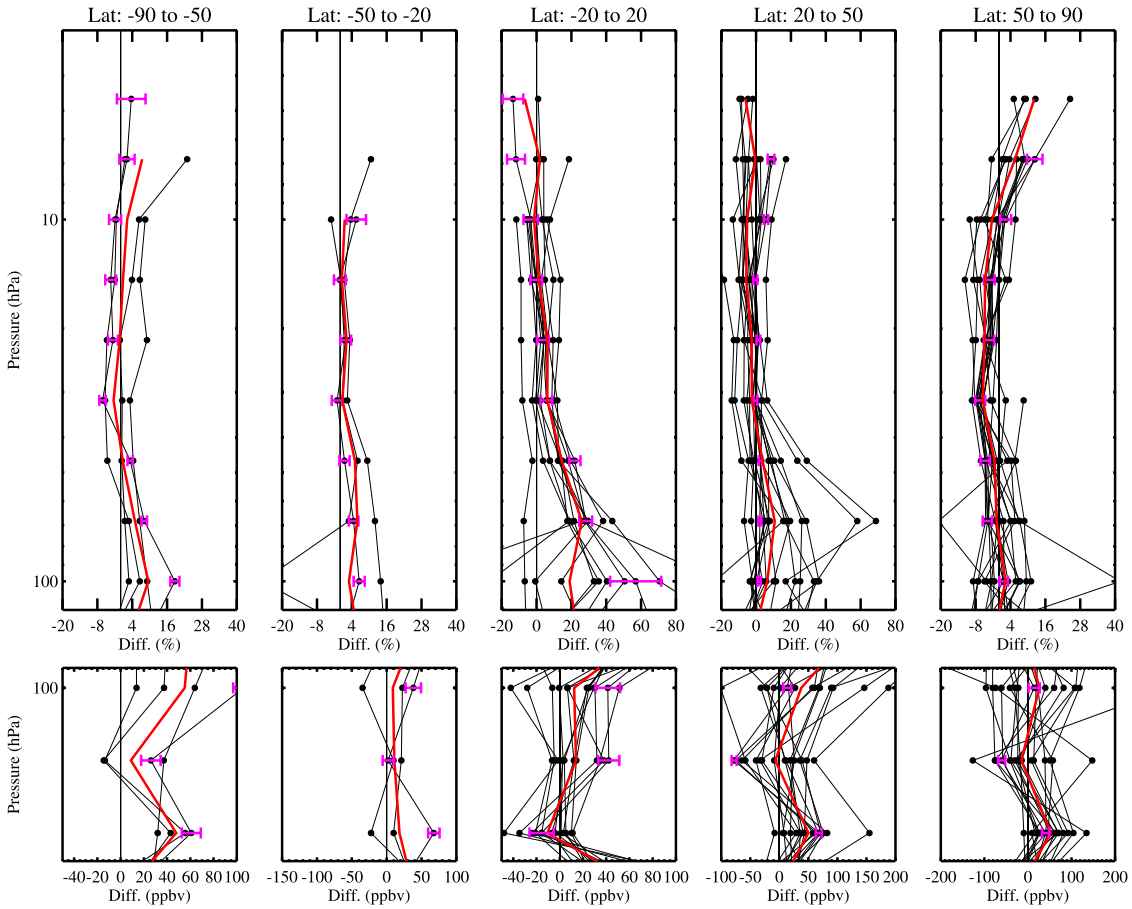

Figure 6. Averaged ozone profiles differences between MLS v2.2 and ozonesondes for each station, in five latitude bins. Profiles at (top) pressure 120–3 hPa and (bottom) at pressure 250–80 hPa. Red lines show the mean of the difference. Note that the differences are given in ppbv for the upper troposphere/lower stratosphere region (Figure 6, bottom) and as a percentage for the stratosphere (Figure 6, top). The error bars (pink) are examples of the 2σ combined precisions for sites Syowa, Lauder, Hawaii, Hohenpeissenberg and De Bilt, in their respective latitude bins. Precisions in the averages for each bin (red curves) are even smaller (and are not shown).

climatology at 147 hPa level as compared to 100 hPa and 215 hPa levels. The differences at 147 hPa have some seasonal variability in the tropical and midlatitude regions with some biases as high as ~20%.

[15] Figure 3 shows comparisons between MLS v2.2 and LLM climatology in 6 latitude bins. MLS ozone values are generally within ~5% of LLM data down to 50 hPa, although there are some larger differences at high southern latitudes. Better agreement is reached in the Northern Hemisphere stratosphere. The standard deviations (variability) of MLS and LLM climatology (not shown here) track very well in the stratosphere, but they deviate from each other in the upper troposphere and lower stratosphere. In the upper troposphere, the standard deviation of MLS is about twice as large as that of the LLM climatology.

[16] As pointed out by Froidevaux et al. (submitted manuscript, 2007), improved algorithms in MLS v2.2 ozone have generally led to reduced biases in comparison to MLS v1.5. For example, MLS v2.2 has largely corrected the small negative slope that existed in v1.5 comparisons with SAGE II. Figure 4 shows the average differences (defined as 100 * (MLS-Sonde)/Sonde) between ozonesonde profiles and MLS v2.2 and v1.5 data (for the same days) for six different latitude bins. MLS v2.2 data show better agreement with ozonesonde values than the MLS v1.5 data in the stratosphere (100–5 hPa). The MLS v2.2 data and ozonesonde data agree with each other from 50 to 5 hPa to within ~5% except in the tropics where ~15% positive bias is observed at 50 hPa. MLS v2.2 profiles still show mostly high biases compared to ozonesondes in the lower altitude range. MLS and ozonesonde values are within ~12% at 100 and 147 hPa except in the tropical latitude bin −20° to 20° where the bias is ~20%. At 215 hPa, MLS ozone is higher by 20% to 35% compared to ozonesondes in extratropical latitudes, but lower by 14% in the tropics. In most latitude bins, the comparisons still show a negative slope from the upper troposphere to about 10 hPa. This plot also shows that the comparisons between MLS and ozonesondes are quite somewhat different from the climatology comparisons (dark gray lines). The combined precision estimate (heavy solid line in Figure 4) is obtained from the root sum square (rss) of the (random) uncertainties provided in the MLS data files and the 5% precision assumed for ozonesonde measurements. The standard deviations of the differences (dashed

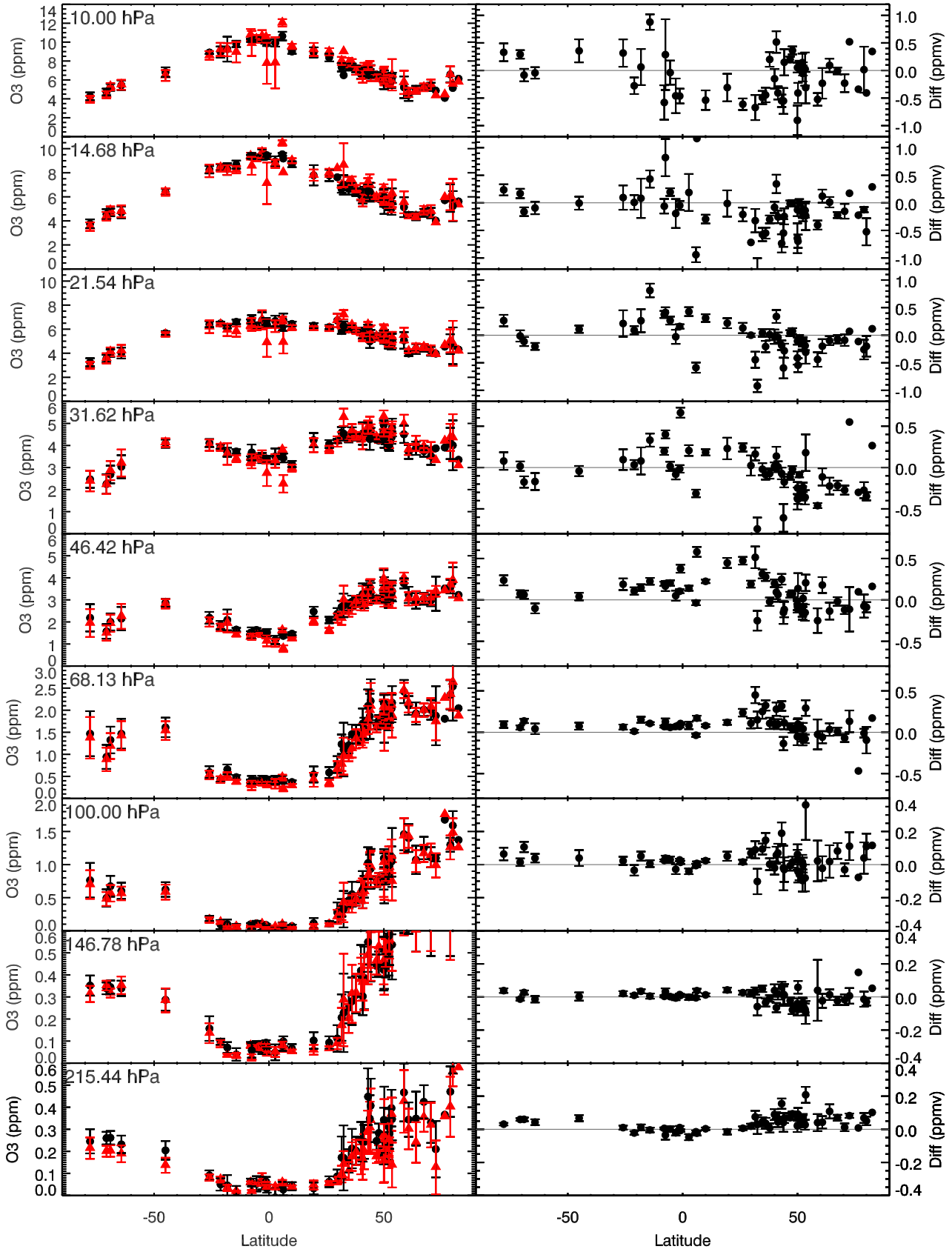

Figure 7. (left) Latitudinal distributions of average ozone from each ozonesonde station (red triangles) compared with MLS ozone data (black dots) on selected pressure levels, as indicated. The error bars are the standard deviation (variability). (right) Differences (MLS minus sonde data) in ppmv. The error bars show twice the standard error in the mean differences.

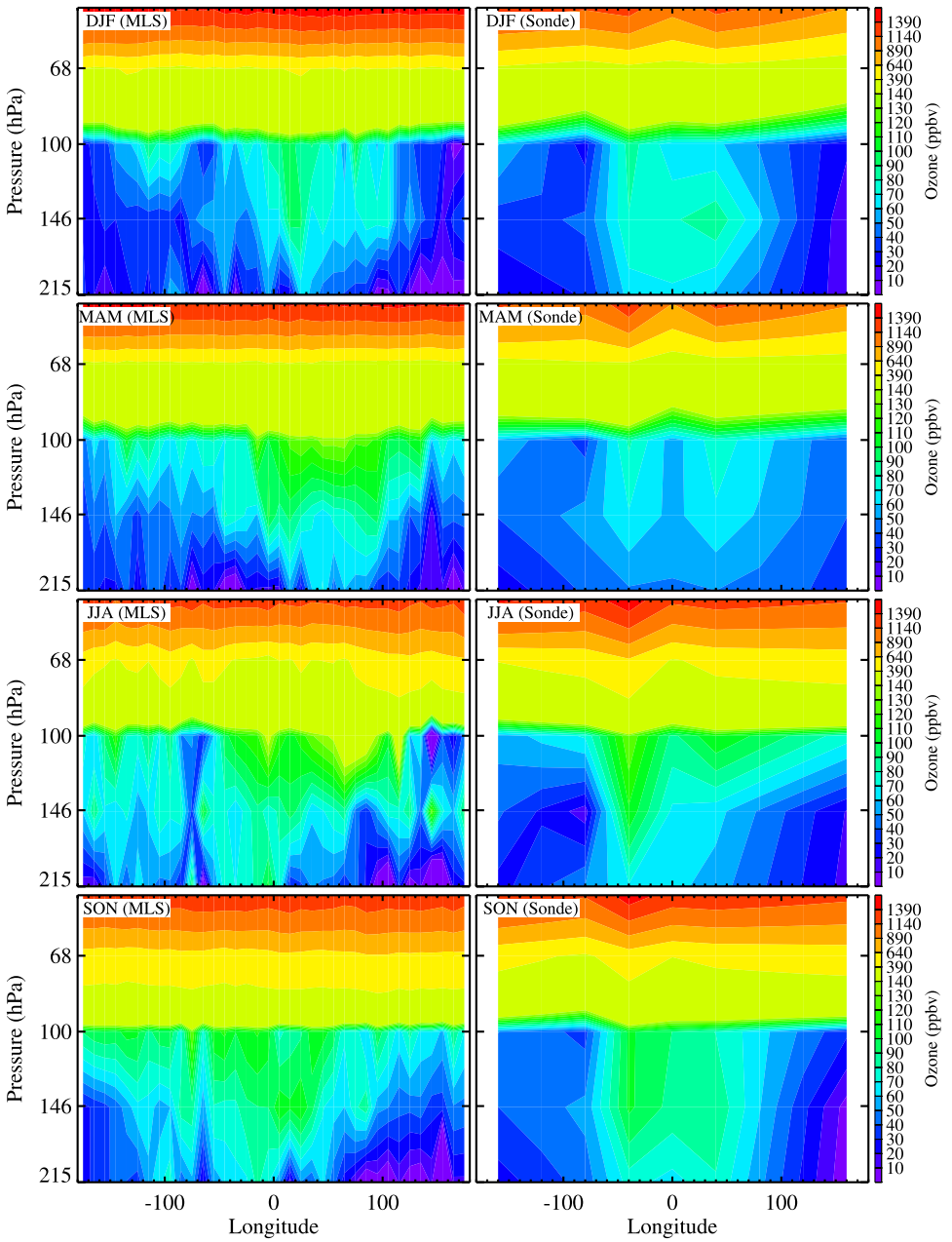

Figure 8. Ozone vertical distribution from 20 hPa to 215 hPa in the equatorial region (±15° in latitude) for four seasons (months indicated by first letters at top left for each panel), using 2004 and 2005 data. (left) From the MLS v1.5 ozone data available and (right) from the ozonesonde measurements in 2004 and 2005, which mostly come from the SHADOZ network.

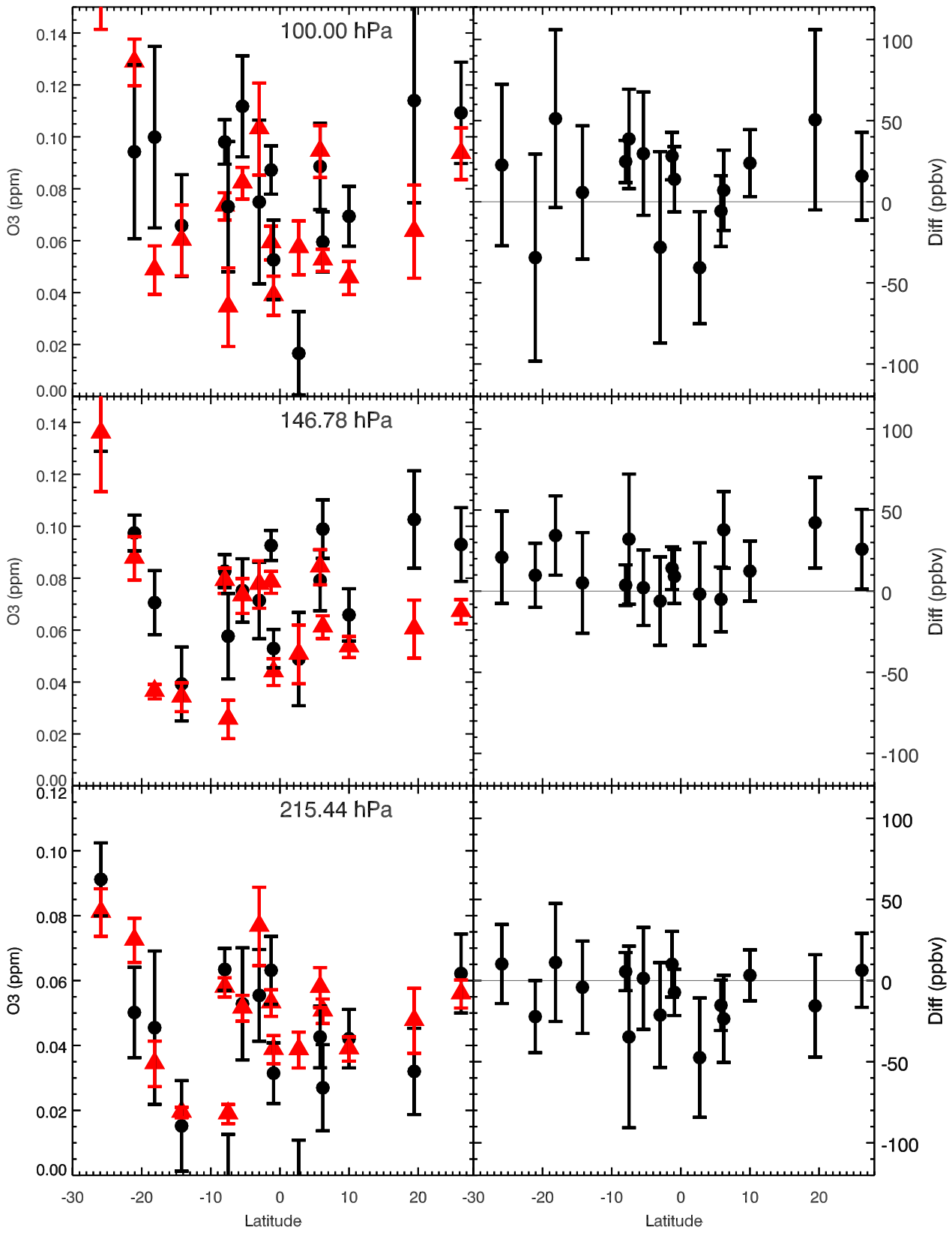

Figure 9. (left) Latitudinal distributions of averaged ozone at each low-latitude ozonesonde station (red triangles), with the standard deviation (variability) shown as error bars (red bar), compared with MLS ozone data (black dots) and their error bars (black bar) at three pressure levels. (right) Differences (MLS minus ozonesonde data) in ppbv. The error bars show twice the standard error in the mean differences.

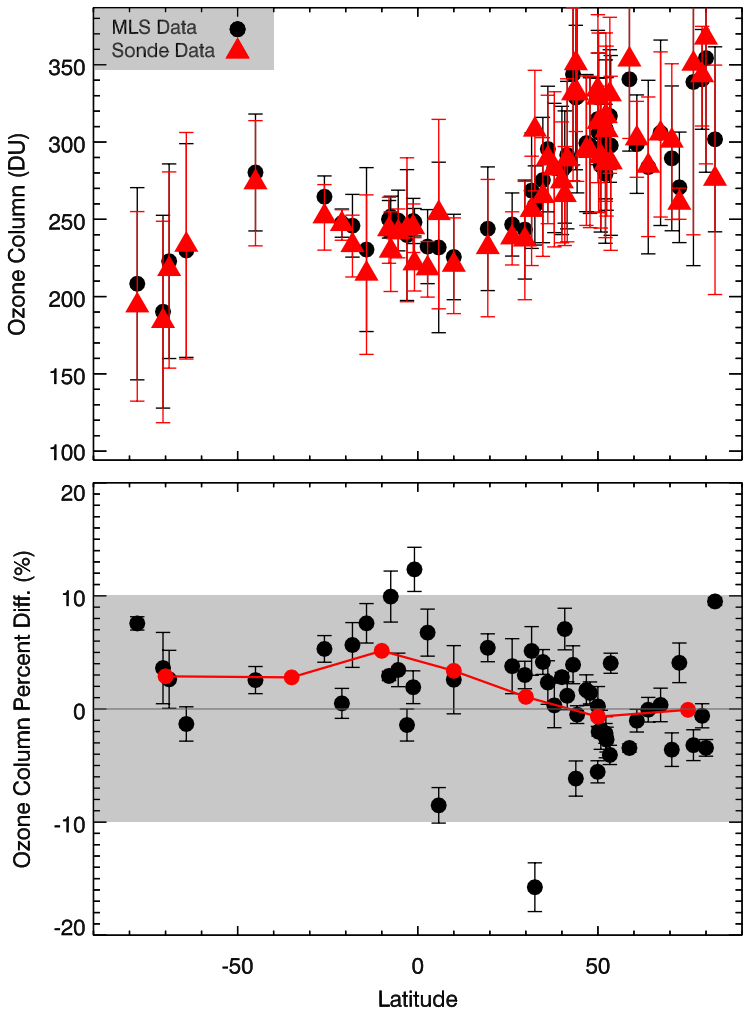

Figure 10. (top) Averaged column ozone at each station as compared with MLS ozone data and (bottom) their differences in percentage. In Figure 10 (top), the black circles are the MLS column ozone with the standard deviation (variability) and ozonesonde columns are represented by red triangles with the standard deviation (variability). Figure 10 (bottom) shows column differences between MLS ozone and ozonesondes with twice the standard error in the mean differences. The (connected) red dots represent the averaged differences over 20° latitude bins in the Northern Hemisphere and 30° latitude bins in the Southern Hemisphere.

line in Figure 4) are larger than these combined precision estimates, especially in the UT/LS. While atmospheric variability could play some role in the larger UT/LS scatter, we also noted this larger variability versus the LLM climatology, and this is a topic for further study. The larger differences (absolute and scatter) in the UT/LS may be caused by the sensitivity of the retrieval in that region, since the ozone in that region only contributes a very small fraction of the total MLS ozone signal. We note that the formal accuracy estimates for MLS ozone in the upper troposphere [*Livesey et al.*, 2007] are larger than the average difference observed in Figure 5.

[17] The MLS v2.2 ozone abundances are well correlated with the ozonesonde values at all pressure levels except at 316 hPa, as shown in Figure 5. The 316 hPa level ozone varies between −0.2 ppmv to 0.4 ppmv, and is not recommended for scientific use. There are a few questionable profiles (outliers) at various levels. Figure 6 presents averaged difference (100 * (MLS-sonde)/sonde) profiles for each station grouped by latitude bin. The largest differences are at lower altitudes. Most of the averaged profiles (from each site) agree with MLS within ∼10% in the midstratosphere. There are some larger, unexplained differences for some sites. In the tropical upper troposphere, most differences are within 30 ppbv, and the average is within ∼10 ppbv. The MLS accuracy estimates in this region is ∼20 ppbv [*Livesey et al.*, 2007].

[18] Figure 7 summarizes the MLS and ozonesonde averaged comparisons for each site versus latitude, with abundances on Figure 7 (left) and differences on Figure 7 (right). The MLS data track the ozonesonde data very well as a function of latitude. Both data sets show smaller ozone mixing ratios in the equatorial region and larger ozone at middle-to-high latitude from 215 hPa to 46 hPa, with a change in the sign of this latitudinal gradient from 21 to 10 hPa. This consistent picture points to the robustness of

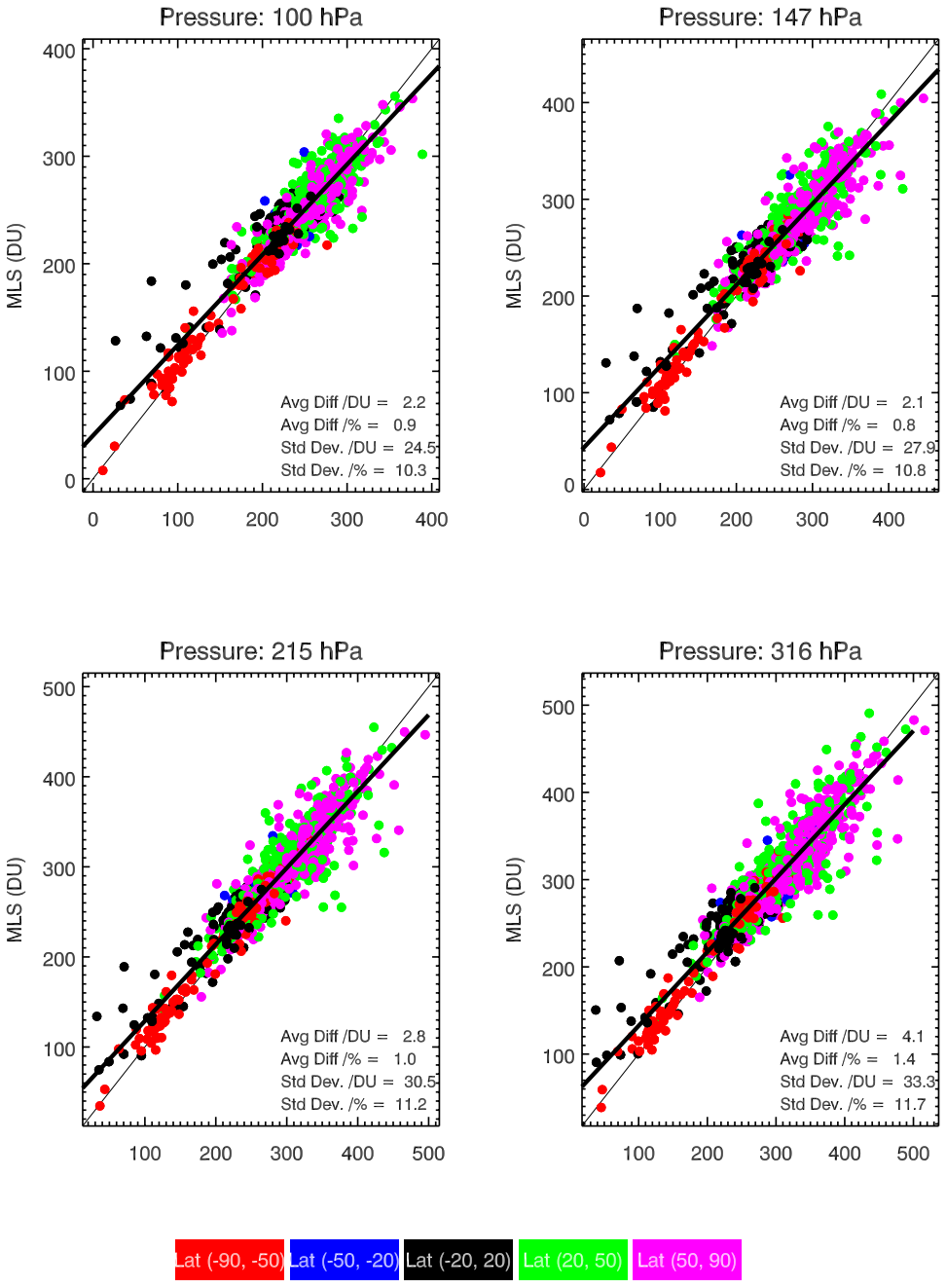

Figure 11. Scatterplots of MLS ozone columns versus ozonesonde columns above four selected pressure levels from all the stations for all the coincidences, color-coded in five latitude bins. The heavy black lines are the linear fits to the data.

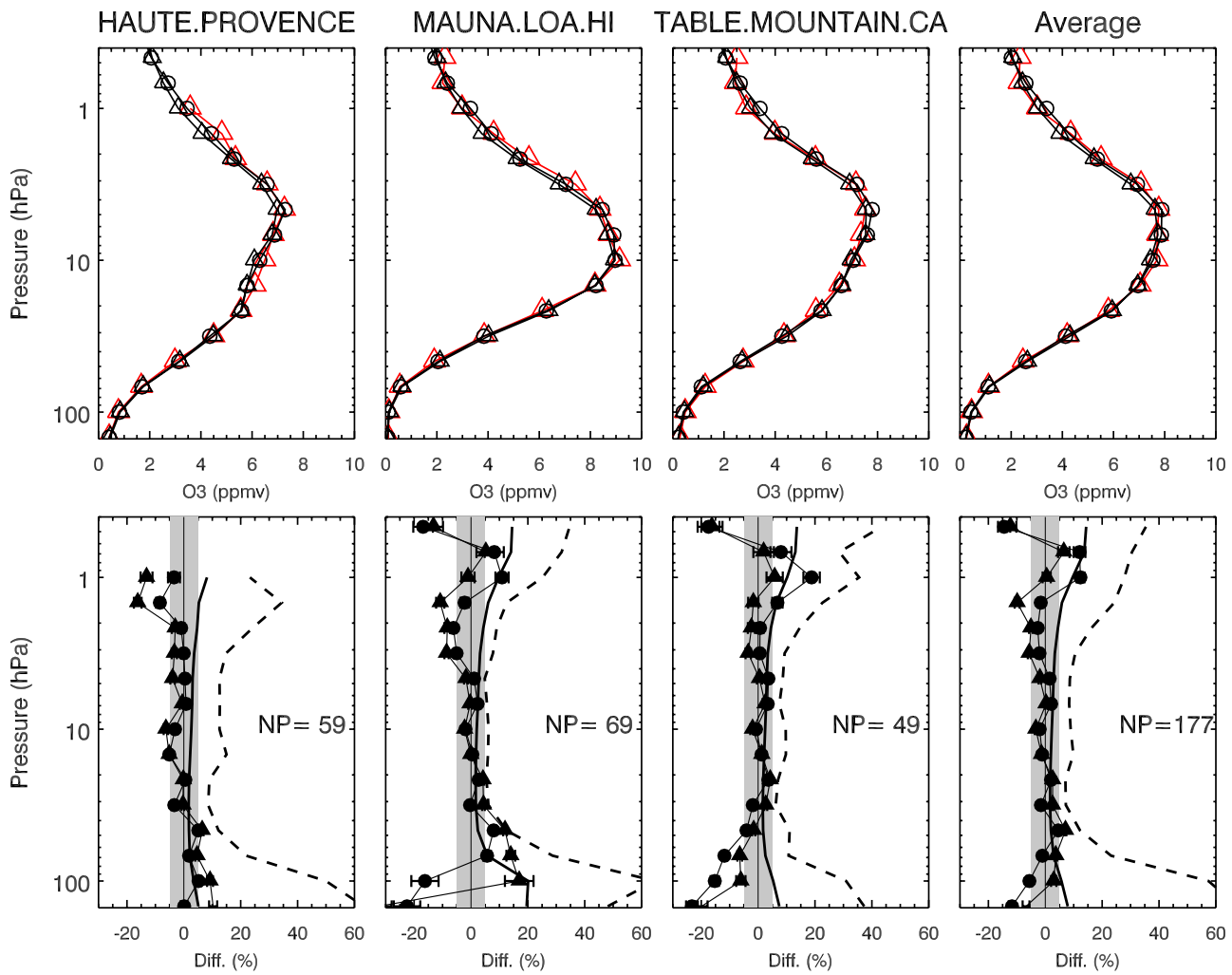

Figure 12. Comparisons between MLS v2.2, v1.5 ozone and lidar measurements at three stations. (top) Averaged profiles of MLS v2.2 (open circles), v1.5 (open triangles) and lidar (open red triangles). (bottom) Average percentage differences between MLS v2.2 and lidar data (solid circles) and the average percentage differences between MLS v1.5 and lidar data (solid triangles). Error bars represent twice the precision (standard error) in these mean differences. Dashed lines give the standard deviations of the mean differences between v2.2 and lidar data. Heavy solid line shows the combined precisions for the v2.2 and lidar measurements. The shaded area is the ±5% region.

the MLS v2.2 retrievals even for the upper troposphere, where ozone contributes only a small fraction to the total emission. The small ozone mixing ratios (<100 ppbv) in the equatorial region below 100 hPa level represent typical upper tropospheric ozone values, and will be examined in more detail in Figure 9.

[19] As presented in Figure 7 (right), the differences between MLS and ozonesondes are less than 100 ppbv for most of the stations in the upper troposphere and lower stratosphere (100 hPa to 215 hPa), and differences tend to oscillate between positive and negative values. The differences are large at stations in the tropical region and north of 30°N for all pressure levels.

[20] Tropospheric pollution and the global effects of regional pollution have received increased attention in the past decade. Tropospheric ozone is a precursor of OH radicals and as such influences tropospheric chemistry and global climate change. Ozone distribution in UT/LS is the result of a combination of transport and chemical processes. The zonal wave one in the tropical distribution of ozone and the tropical Atlantic ozone paradox [*Thompson et al.*, 2003; *Sauvage et al.*, 2006] are interesting examples of variations in tropospheric ozone, and better characterization of the spatial and temporal variations of tropospheric ozone is needed.

[21] The well-known enhancements in tropospheric ozone over the tropical Atlantic (∼165–90°W in longitude) [*Thompson et al.*, 2003; *Jourdain et al.*, 2007] are shown both in the MLS ozone data and in the ozonesonde measurements (Figure 8) in December, January, and February (DJF) and March, April, and May (MAM). This phenomenon appears to be associated with pollution from biomass burning in Africa and South America and the tropical circulation. Moreover, MLS data also show enhanced ozone

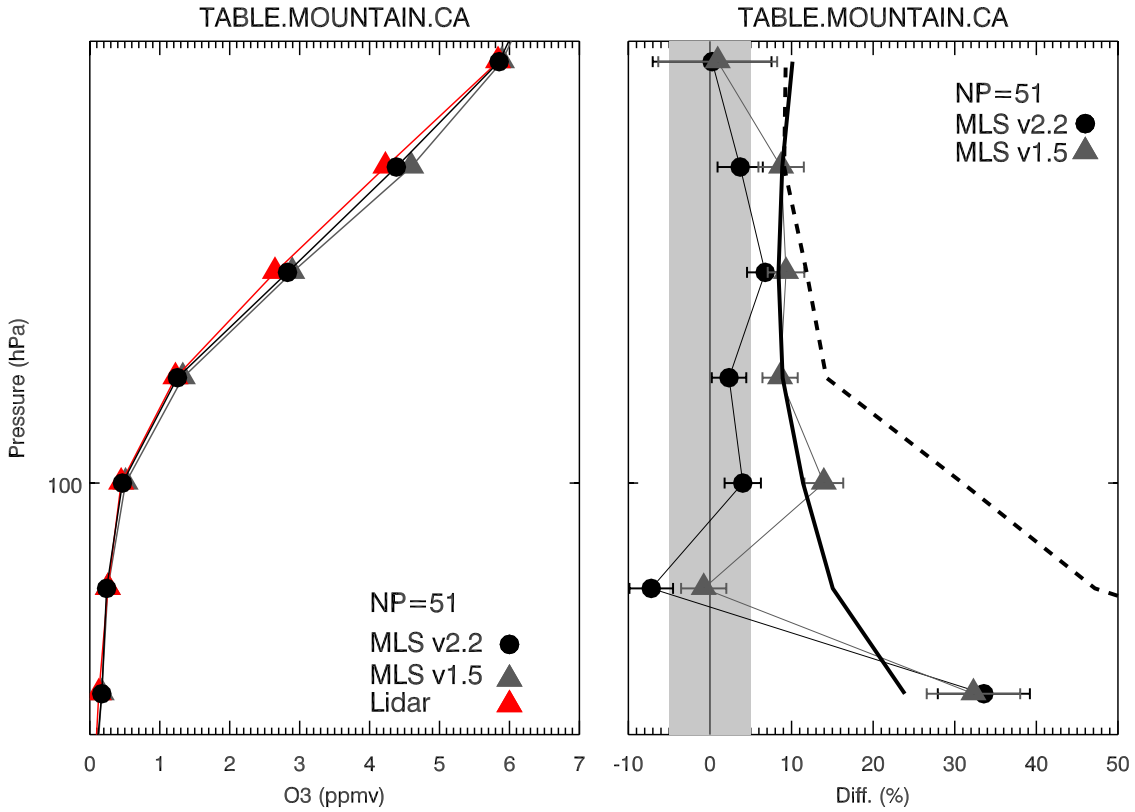

Figure 13. Same as Figure 12 except that the lidar data are from the Table Mountain Facility tropospheric ozone measurements; and the pressure levels are from 215 to 22 hPa.

in the tropical Pacific (~35°W–8°E in longitude) in June, July, and August (JJA), and in September, October, and November (SON), which may not appear in ozonesonde measurements because of their sparse coverage. The higher ozone in the tropical Pacific in JJA and SON may also be caused by biomass burning, followed by cross-continental transport of polluted air lofted into the upper troposphere. There is also the possibility that stratosphere-troposphere exchange plays a role. The lower stratosphere ozone in the tropical region is relatively uniform longitudinally and shows no signal of the tropospheric wave one pattern.

[22] Figure 9 shows the comparisons in detail in the equatorial region at 215 hPa, 147 hPa and 100 hPa in the upper troposphere. The averaged differences for each station are within 50 ppbv at 215, 146 and 100 hPa, although there is significant variability from site to site. The standard errors are within about 30 ppbv, which is roughly consistent with the results of analyses by *Livesey et al.* [2007], using aircraft data sources. There is slightly significant bias in the tropical upper tropospheric comparisons (see Figure 4). The 215 hPa high bias of ~20% seen in Figure 4 arises mainly from the middle and high latitudes (south of −20° and north of 20°).

[23] Ozone column abundance is another parameter of interest used in the process of validating MLS data against ozonesonde measurements. The MLS column ozone abundances are estimated to have a (1σ) precision of 3%, for a typical column value obtained from the integration of an individual MLS ozone profile (Froidevaux et al., submitted manuscript, 2007), with an estimated (2σ) accuracy of 4% (or 8 DU). Comparisons of column ozone measurements from MLS and column data from the CCD based Actinic Flux Spectroradiometers (CAFS) during various Aura Validation Experiment (AVE) campaigns (N. J. Petropavlovskikh et al., Validation of Aura Microwave Limb Sounder O_3 and CO observations in the upper troposphere and lower stratosphere, manuscript in preparation, 2007) confirm that such uncertainty estimates are reasonable, as do column comparisons between MLS and other satellite-based ozone measurements (Froidevaux et al., submitted manuscript, 2007; Yang et al., submitted manuscript, 2007). Figure 10 gives the averaged ozone partial column from MLS v2.2 data and ozonesonde partial column from each station, and the differences. The MLS ozone partial column and ozonesonde partial column are calculated between common upper and lower pressure levels where good measurements are made for both MLS and ozonesondes. As seen in Figure 7, the ozone partial columns also show good correspondence in the meridional variations, and the mean differences are mostly within 10% with a few fliers. Typically, twice the standard error shown in Figure 10 is about 3%.

[24] More detailed partial column ozone scatterplots of MLS versus ozonesonde partial column ozone above four selected pressure levels are shown in Figure 11; different latitude bins are color-coded in this plot. There is a 1.4% average difference (MLS values higher than sonde values) for columns above 316 hPa, and this difference decreases as pressure decreases. The correlation coefficients for all

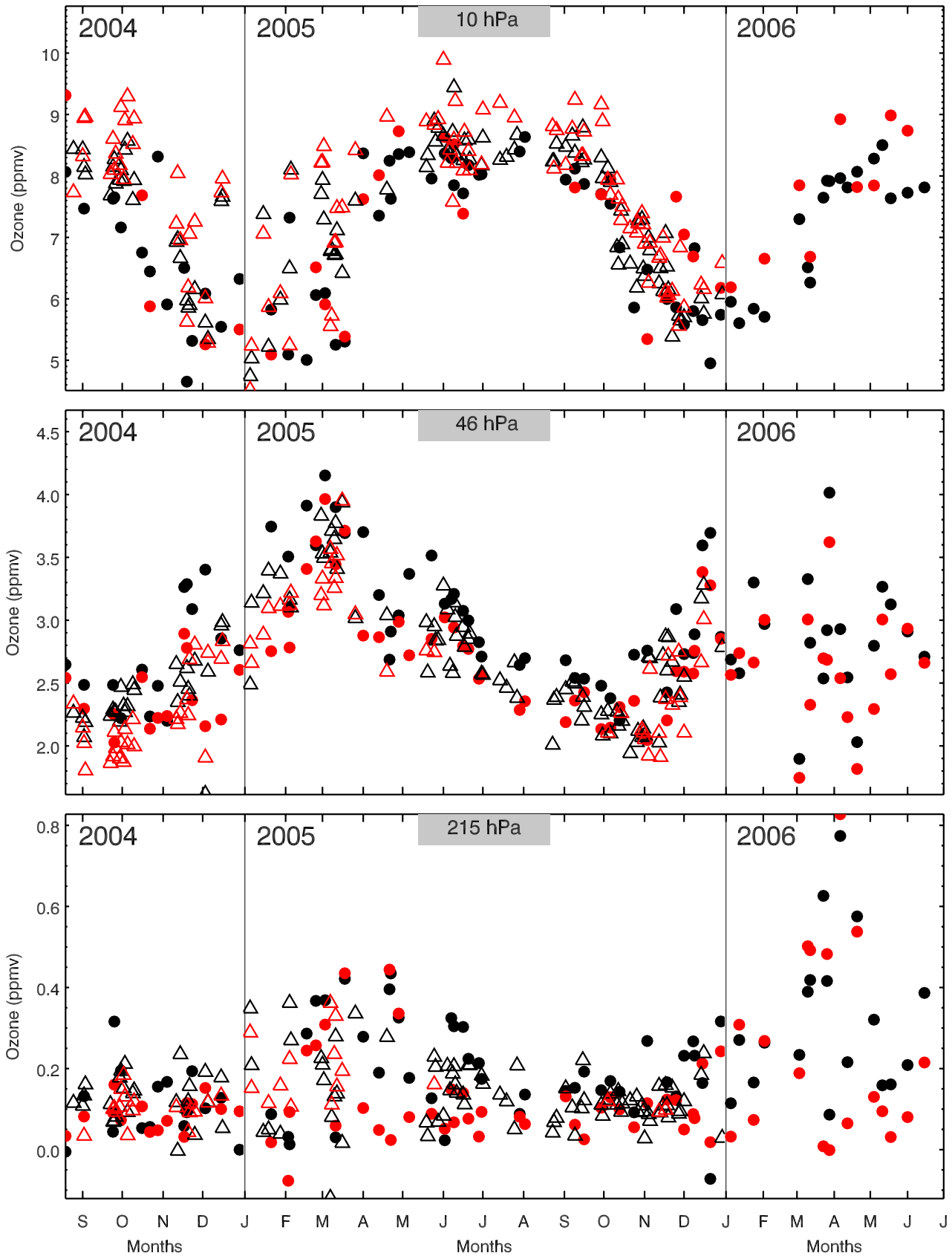

Figure 14. Time series comparisons between MLS v2.2 ozone (black open triangle) and lidar (red open triangle) measurements at Table Mountain and between MLS v2.2 ozone (black dot) and ozonesonde (red dot) measurements at Boulder, Colorado, in 2004, 2005 and 2006 at three selected pressure levels (10, 46, and 215 hPa).

Table 3. Summary of Comparisons Between MLS Ozone and Ozonesonde Data (Global)

Pressure, hPa	Difference With Sonde, %	Combined Precision, %	Standard Deviation of Difference, %
215.4	22	15	64
146.8	−5	8	40
100.0	2	7	40
<100 and >5	5	5	10

pressure levels are about 0.95; MLS column ozone in the tropics shows larger biases, as expected from this Figure 10.

4. Comparisons of MLS Versus Lidar Ozone Data

[25] We have analyzed comparisons between MLS ozone and ozone from four lidars located at three NDACC (Network for the Detection of Atmospheric Composition Change, formerly NDSC) stations [*Leblanc and McDermid*, 2000; *Leblanc et al.*, 2006; *McDermid et al.*, 1990; *Godin et al.*, 1989; *Godin-Beekmann et al.*, 2003], namely Observatoire de Haute-Provence (OHP) in France (43.93°N, 5.71°E), Mauna Loa, Hawaii (19.5°N, 155.7°W), and the Table Mountain Facility, California (34.5°N, 117.7°W). These lidars are high power differential absorption lidars (or DIAL) which make precise measurements of stratospheric ozone concentration profiles from ~20 to 50 km altitude. This technique requires two (or more) laser wavelengths which are chosen such that one coincides with a region of high absorption, specific to the species being measured, and the other is tuned into the wings of this feature to a wavelength with much lower absorption. The concentration of ozone is retrieved by measuring the different absorption of the backscatter data at the two wavelengths.

[26] The estimated accuracy (or systematic uncertainty) for the Table Mountain Facility ozone number density lidar profiles is below 0.05×10^{18} molecules/m^3 (or 1–5%) for the vertical range 15–50 km and can occasionally increase to 0.3×10^{18} molecules/m^3 (or 10–50%) for heights below 15 km. The translation to mixing ratio adds another 1–3% uncertainty due to the use (and associated uncertainty) of external measurements or model outputs of pressure and temperature. The temperature and pressure data used for OHP correspond to nearby radiosoundings performed daily in Nimes, complemented at higher altitude by the COSPAR International Reference Atmosphere (CIRA) [*Rees*, 1988] model. Hawaii and Table Mountain lidars use National Centers for Environmental Prediction (NCEP) operational analysis data interpolated to the location and time of the lidar measurements, and local Hilo radiosondes complement the Hawaii database. In this validation study against lidar measurements, we have degraded the high-resolution lidar profiles to MLS data grid by using the averaging kernel method as pointed out in section 3.

[27] Figure 12 shows the averaged profiles of available MLS v2.2 data and coincident lidar measurements (within ±2° latitude, ±10° longitude and for nighttime only) and their percentage differences (defined as 100 * (MLS-lidar)/lidar) at the three lidar stations. The comparisons with the tropospheric ozone lidar measurements at Table Mountain Facility are discussed later. MLS v2.2 shows better agreement with lidar data than v1.5. MLS v2.2 ozone gives best agreement with lidar in the 2 hPa to 50 hPa region, where the differences are within 5%. The relatively larger differences (>10%) around 1 hPa and higher, for all three stations, may be caused by poorer lidar measurements in this region. For the Haute Provence station, averaged differences are less than 5% at 100 and 146 hPa, and 20% at 215 hPa. At 147 hPa, MLS v2.2 ozone is lower by ~20% (uncertainty 10%) compared to both the Mauna Loa and the Table Mountain Facility measurements. On average, on the basis of these three stations, MLS v2.2 agrees with lidar measurements to better than ~5% from 5 hPa to 100 hPa. The comparisons also show larger standard deviations of the mean differences for pressures of 100 hPa and larger. Calculations of partial column ozone abundances above 215 hPa over the three lidar stations indicate that MLS v2.2 data agree with the lidars to better than 5%.

[28] Figure 13 shows the comparisons between MLS low altitude ozone and that measured by the Table Mountain tropospheric ozone lidar. The tropospheric ozone lidar measurement system provides a more reliable comparison for this altitude region in the upper troposphere. The differences between MLS v2.2 ozone and lidar are within 8% down to 147 hPa, but MLS shows a high bias (~30%) at 215 hPa, which is consistent with the ozonesonde measurements. The estimated combined precision is about 10% at pressures less than 100 hPa and increases to ~25% for pressures larger than 100 hPa. The standard deviations of the mean differences (dashed lines) are higher than 10% and increase to more than 50% in the upper troposphere. Figure 13 also highlights the better agreement versus lidars for MLS v2.2 than MLS v1.5 data in the stratosphere.

[29] In Figure 14, we present the time series of MLS ozone, ozonesonde measurements at Boulder, Colorado and lidar measurements at Table Mountain Facility in 2004, 2005 and 2006 at three pressure levels. The tropospheric lidar measurement is used at 215 hPa level in the comparison. These two stations are the closest stations we can find for the comparisons of the three different kinds of measurements, and they should have similar spatial and temporal ozone variability. In general, the MLS v2.2 ozone tracks both the ozonesonde and lidar measurements well as a function of season. The ozone abundance at 215 hPa shows a weak seasonal variability with enhanced values around spring, but shows a strong seasonal cycle at both 46 and 10 hPa. The ozone distribution reaches its maximum in the

Table 4. Summary of Comparisons Between MLS Ozone and Lidar Data[a]

Pressure, hPa	Difference With Lidar, %	Combined Precision, %	Standard Deviation of Differences, %
215.4	34	23	80
146.8	−7	15	32
100.0	4	11	30
<100 and >5	5	10	15

[a]Table Mountain Tropospheric Lidar is used here at levels from 100 hPa to 215 hPa, and other lidar measurements are used for pressure levels between 5 hPa and 100 hPa.

summer at 10 hPa, while it reaches its maximum in the spring at 46 hPa.

5. Summary and Conclusions

[30] This paper presents the validation results of newly released Aura MLS v2.2 ozone in the upper troposphere and lower stratosphere using worldwide ozonesonde and ground-based lidar measurements. In the upper troposphere and lower stratosphere, MLS ozone is generally biased high at middle to high latitudes, as compared to ozonesondes, but within 20% or 20 ppbv, on average, in the tropics. In the middle stratosphere, MLS is within 7% of the global ozonesonde measurements. Averaged over each ozonesonde station, the column ozone comparisons against MLS show better than 10% agreement, but there is no significant bias globally.

[31] Comparisons to three sets of lidar measurements from Hawaii, Table Mountain, and Haute Provence in France show excellent agreement (within about 5%) in the stratosphere and MLS ozone biases higher by 35% at 215 hPa level. This study also shows that the temporal variations in MLS ozone and in midlatitude ozone from the Boulder, CO, ozonesondes and the Table Mountain Facility, CA, lidar track each other very well. The global results of comparisons between ozonesondes and lidars are listed in Tables 3 and 4. The results from the lidar comparisons are consistent with that from the ozonesonde comparisons in the lower altitude range. However, the comparisons between MLS ozone and aircraft in situ and lidar data do not give strong evidence for a high MLS bias at 215 hPa of more than 15% [*Livesey et al.*, 2007; Froidevaux et al., submitted manuscript, 2007]. Because of the somewhat inconsistent evidence of a high MLS bias at 215 hPa, the accuracy estimate for MLS v2.2 ozone at 215 hPa has been set at about 20 ppbv + 20% (see the above references), rather than the somewhat lower estimate of 20 ppbv + 10% expected from simulations and sensitivity studies (see the above two references). Further detailed investigations using more reprocessed MLS v2.2 data may shed more light on these issues.

[32] **Acknowledgments.** This work at the Jet Propulsion Laboratory, California Institute of Technology, was performed under contract with NASA. We are very grateful to the MLS instrument and data/computer operations and development team (at JPL and from Raytheon, Pasadena) for their support through all the phases of the MLS project, in particular D. Flower, G. Lau, J. Holden, R. Lay, M. Loo, G. Melgar, D. Miller, B. Mills, M. Echeverri, E. Greene, A. Hanzel, A. Mousessian, S. Neely, C. Vuu, and P. Zimdars. We greatly appreciate the work of those involved in the Aura Validation Data Center at the NASA Goddard Space Flight Center, as this has been the main data repository for Aura correlative/validation data since the Aura launch. Thanks to Jennifer Logan for providing the WOUDC data. Thanks to the Aura Project for their support throughout the years (before and after the Aura launch), in particular M. Schoeberl, A. Douglass (also as cochair of the Aura validation working group), E. Hilsenrath, and J. Joiner. We also acknowledge the support from NASA Headquarters; P. DeCola for MLS and Aura; and M. Kurylo, J. Gleason, B. Doddridge, and H. Maring, especially in relation to the Aura validation activities and campaign planning efforts.

References

Bodeker, G. E., I. S. Boyd, and W. A. Matthews (1998), Trends and variability in vertical ozone and temperature profiles measured by ozonesondes at Lauder, New Zealand: 1986–1996, *J. Geophys. Res.*, *103*(D22), 28,661–28,681.

Borchi, F., J.-P. Pommereau, A. Garnier, and M. Pinharanda (2005), Evaluation of SHADOZ sondes, HALOE and SAGE II ozone profiles at the tropics from SAOZ UV-Vis remote measurements onboard long duration balloons, *Atmos. Chem. Phys.*, *5*, 1381–1397.

Froidevaux, L., et al. (2006), Early validation analyses of atmospheric profiles from EOS MLS on the Aura satellite, *IEEE Trans. Geosci. Remote Sens.*, *44*(5), 1106–1121.

Godin, S., G. Mégie, and J. Pelon (1989), Systematic Lidar Measurements of the Stratospheric Ozone Vertical Distribution, *Geophys. Res. Lett.*, *16*(6), 547–550.

Godin-Beekmann, S., J. Porteneuve, and A. Garnier (2003), Systematic DIAL ozone measurements at Observatoire de Haute-Provence, *J. Environ. Monit.*, *5*, 57–67.

Hocke, K., N. Kampfer, D. G. Feist, H. Calisesi, J. H. Jiang, and S. Chabrillat (2006), Temporal variance of lower mesospheric ozone over Switzerland during winter 2000/2001, *Geophys. Res. Lett.*, *33*, L09801, doi:10.1029/2005GL025496.

Johnson, B. J., S. J. Oltmans, H. Vomel, H. G. J. Smit, T. Deshler, and C. Kroger (2002), Electrochemical concentration cell (ECC) ozonesonde pump efficiency measurements and tests on the sensitivity to ozone of buffered and unbuffered ECC sensor cathode solutions, *J. Geophys. Res.*, *107*(D19), 4393, doi:10.1029/2001JD000557.

Jourdain, L., et al. (2007), Tropospheric vertical distribution of tropical Atlantic ozone observed by TES during the Northern African biomass burning season, *Geophys. Res. Lett.*, *34*, L04810, doi:10.1029/2006GL028284.

Kerr, J. B., et al. (1994), The 1991 WMO international ozonesonde intercomparison at Vanscoy, Canada, *Atmos. Ocean*, *32*, 685–716.

Leblanc, T., and I. S. McDermid (2000), Stratospheric ozone climatology from Lidar measurements at Table Mountain (34.4°N, 117.7°W) and Mauna Loa (19.5°N, 155.6°W), *J. Geophys. Res.*, *105*, 14,613–14,623.

Leblanc, T., O. P. Tripathi, I. S. McDermid, L. Froidevaux, N. J. Livesey, W. G. Read, and J. W. Waters (2006), Simultaneous lidar and EOS MLS measurements, and modeling, of a rare polar ozone filament event over Mauna Loa Observatory, Hawaii, *Geophys. Res. Lett.*, *33*, L16801, doi:10.1029/2006GL026257.

Livesey, N. J., et al. (2005), EOS MLS version 1.5 Level 2 data quality and description document, *Tech. Rep. D-32381*, Jet Propul. Lab., Pasadena, Calif.

Livesey, N. J., et al. (2006), Retrieval algorithms for the EOS Microwave Limb Sounder (MLS), *IEEE Trans. Geosci. Remote Sens.*, *44*(5), 1144–1155.

Livesey, N. J., et al. (2007), Validation of Aura Microwave Limb Sounder O_3 and CO observations in the upper troposphere and lower stratosphere, *J. Geophys. Res.*, doi:10.1029/2007JD008805, in press.

McDermid, I. S., S. M. Godin, and T. D. Walsh (1990), Lidar measurements of stratospheric ozone and intercomparisons and validation, *Appl. Opt.*, *29*, 4914–4923.

McPeters, R. D., G. J. Labow, and J. Logan (2007), Ozone climatological profiles for satellite retrieval algorithms, *J. Geophys. Res.*, *112*, D05308, doi:10.1029/2005JD006823.

Read, W. G., Z. Shippony, M. J. Schwartz, N. J. Livesey, and W. V. Snyder (2006), The clear-sky unpolarized forward model for the EOS Microwave Limb Sounder (MLS), *IEEE Trans. Geosci. Remote Sens.*, *44*(5), 1367–1379.

Rees, D. (Ed.) (1988), *CIRA 1986*, *Adv. Space Res.*, *8* (5–6).

Rodgers, C. D. (1976), Retrieval of atmospheric temperature and composition from remote measurements of thermal radiation, *Rev. Geophys.*, *14*, 609–624.

Sauvage, B., V. Thouret, A. M. Thompson, J. C. Witte, J.-P. Cammas, P. Nedelec, and G. Athier (2006), Enhanced view of the "tropical Atlantic ozone paradox" and "zonal wave one" from the in situ MOZAIC and SHADOZ data, *J. Geophys. Res.*, *111*, D01301, doi:10.1029/2005JD006241.

Schoeberl, M. R., et al. (2006a), Overview of the EOS Aura mission, *IEEE Trans. Geosci. Remote Sens.*, *44*(5), 1066–1074.

Schoeberl, M. R., et al. (2006b), Chemical observations of a polar vortex intrusion, *J. Geophys. Res.*, *111*, D20306, doi:10.1029/2006JD007134.

Schwartz, M. J., W. G. Read, and W. Van Snyder (2006), EOS MLS forward model polarized radiative transfer for Zeeman-split oxygen lines, *IEEE Trans. Geosci. Remote Sens.*, *44*, 1182–1191.

Smit, H. G. J., et al. (2007), Assessment of the performance of ECC-ozonesondes under quasi-flight conditions in the environmental simulation chamber: Insights from the Juelich Ozone Sonde Intercomparison Experiment (JOSIE), *J. Geophys. Res.*, *112*, D19306, doi:10.1029/2006JD007308.

Thompson, A. M., et al. (2003), Southern Hemisphere Additional Ozonesondes (SHADOZ) 1998–2000 tropical ozone climatology: 2. Tropospheric variability and the zonal wave-one, *J. Geophys. Res.*, *108*(D2), 8241, doi:10.1029/2002JD002241.

Thompson, A. M., J. C. Witte, H. G. J. Smit, S. J. Oltmans, B. J. Johnson, V. W. J. H. Kirchhoff, and F. J. Schmidlin (2007a), Southern Hemisphere Additional Ozonesondes (SHADOZ) 1998–2004 tropical ozone clima-

tology: 3. Instrumentation, station-to-station variability, and evaluation with simulated flight profiles, *J. Geophys. Res.*, *112*, D03304, doi:10.1029/2005JD007042.

Thompson, A. M., et al. (2007b), Intercontinental Chemical Transport Experiment Ozonesonde Network Study (IONS) 2004: 1. Summertime upper troposphere/lower stratosphere ozone over northeastern North America, *J. Geophys. Res.*, *112*, D12S12, doi:10.1029/2006JD007441.

Thompson, A. M., et al. (2007c), Intercontinental Chemical Transport Experiment Ozonesonde Network Study (IONS) 2004: 2. Tropospheric ozone budgets and variability over northeastern North America, *J. Geophys. Res.*, *112*, D12S13, doi:10.1029/2006JD007670.

Waters, J. W., et al. (1999), The UARS and EOS Microwave Limb Sounder Experiments, *J. Atmos. Sci.*, *56*, 194–218.

Waters, J. W., et al. (2006), The Earth Observing System Microwave Limb Sounder (EOS MLS) on the Aura satellite, *IEEE Trans. Geosci. Remote Sens.*, *44*(5), 1075–1092.

World Climate Research Programme (1998), SPARC/IOC/GAW assessment of trends in the vertical distribution of ozone, stratospheric processes and their role in climate, *Global Ozone Res. Monit. Proj. Rep. 43*, World Meteorol. Organ., Geneva, Switzerland.

Wu, D. L., J. H. Jiang, and C. P. Davis (2006), EOS MLS cloud ice measurements and cloudy-sky radiative transfer model, *IEEE Trans. Geosci. Remote Sens.*, *44*(5), 1156–1165.

Ziemke, J. R., S. Chandra, B. N. Duncan, L. Froidevaux, P. K. Bhartia, P. F. Levelt, and J. W. Waters (2006), Tropospheric ozone determined from Aura OMI and MLS: Evaluation of measurements and comparison with the Global Modeling Initiative's Chemical Transport Model, *J. Geophys. Res.*, *111*, D19303, doi:10.1029/2006JD007089.

M. Allaart and H. Kelder, Royal Netherlands Meteorological Institute, NL-3730 AE de Bilt, Netherlands.

S. B. Andersen, Danish Meteorological Institute, DK-20100 Copenhagen, Denmark.

G. Bodeker, National Institute of Water and Atmospheric Research, Lauder, New Zealand.

B. Bojkov, NASA Goddard Space Flight Center, Greenbelt, MD 20771, USA.

B. Calpini, R. Stubi, and P. Viatte, Aerological Station Payerne, MeteoSwiss, CH-1530 Payerne, Switzerland.

H. Claude, Meteorological Observatory Hohenpeissenberg, German Weather Service, D-82383 Hohenpeissenberg, Germany.

G. Coetzee, South African Weather Service, Irene 0062, South Africa.

R. E. Cofield, D. T. Cuddy, W. H. Daffer, B. J. Drouin, L. Froidevaux, R. A. Fuller, R. F. Jarnot, Y. B. Jiang, B. W. Knosp, A. Lambert, N. J. Livesey, V. S. Perun, W. G. Read, M. J. Schwartz, W. V. Snyder, P. C. Stek, R. P. Thurstans, P. A. Wagner, and J. W. Waters, Jet Propulsion Laboratory, California Institute of Technology, Pasadena, CA 91109, USA. (ybj@mls.jpl.nasa.gov)

J. Davies and D. Tarasick, Environment Canada, Downsview, ON, Canada M3H 5T4.

H. De Backer, Royal Meteorological Institute of Belgium, B-1180 Brussels, Belgium.

H. Dier, Meteorological Observatory Lindenberg, German Weather Service, D-15864 Lindenberg, Germany.

M. J. Filipiak and R. S. Harwood, Institute of Atmospheric and Environmental Science, University of Edinburgh, Edinburgh EH9 3JZ, UK.

L. S. Fook, Malaysian Meteorological Service, Jalan Sultan, 46667 Petaling Jaya, Selangor, Malaysia.

M. Fujiwara, Graduate School of Environmental Earth Science, Hokkaido University, Sapporo 060-0810, Japan.

S. Godin-Beekmann, Service d'Aeronomie/Institut Pierre-Simon Laplace, Centre National de la Recherche Scientifique–Université Pierre et Marie Curie, F-75252 Paris, France.

B. Johnson and S. Oltmans, Global Monitoring Division, Earth System Research Laboratory, NOAA, Boulder, CO 80305, USA.

G. König-Langlo, Alfred Wegener Institute for Polar and Marine Research, D-27515 Bremerhaven, Germany.

E. Kyro, Arctic Research Center, Finnish Meteorological Institute, FIN-99600 Sodankyla, Finland.

G. Laneve, Centro di Ricerca Progetto San Marco, Università degli Studi di Roma "La Sapienza," I-00185 Rome, Italy.

T. Leblanc and I. S. McDermid, Jet Propulsion Laboratory, California Institute of Technology, Table Mountain Facility, Wrightwood, CA 92397, USA.

N. P. Leme, Laboratorio De Ozonio, Instituto Nacional de Pesquisas Espaciais, Sao Paulo 12201-970, Brazil.

J. Merrill, Graduate School of Oceanography, University of Rhode Island, Narragansett, RI 02882, USA.

G. Morris, Department of Physics and Astronomy, Valparaiso University, Valparaiso, IN 46383, USA.

M. Newchurch, Atmospheric Science Department, University of Alabama–Huntsville, Huntsville, AL 35805, USA.

M. C. Parrondos and M. Yela, National Institute for Aerospace Technology, E-28850 Madrid, Spain.

F. Posny, Laboratoire de l'Atmosphère et des Cyclones, F-97715 La Réunion, France.

F. Schmidlin, NASA Goddard Space Flight Center, Wallops Island, VA 23337, USA.

P. Skrivankova, Czech Hydrometeorological Institute, 143 06 Prague, Czech Republic.

A. Thompson, Department of Meteorology, Pennsylvania State University, State College, PA 16802, USA.

V. Thouret, Laboratoire d'Aerologie, Centre National de la Recherche Scientifique, F-31400 Toulouse, France.

H. Vömel, Cooperative Institute for Research in Environmental Science, University of Colorado, Boulder, CO 80309, USA.

P. von Der Gathen, Alfred Wegener Institute, D-14473 Potsdam, Germany.

G. Zablocki, Institute of Meteorology and Water Management, UI Zegrzynska 38, 05-120 Legionowo, Poland.